IIETA International Information and Engineering Technology Association
Advancing the World of Information and Engineering

Annales de Chimie - Science des Matériaux
vol. 49, no. 5, October, 2025, pp. 475-487
Journal homepage: http://iieta.org/journals/acsm

Enhancing Oil-Water Separation: Impact of Nanoparticle Coatings on Quartz Particles

Nthabiseng J. Ramanamane*, Mothibeli Pita

Department of Mechanical Engineering, University of South Africa, Roodepoort 1709, South Africa

Corresponding Author Email: ramannj@unisa.ac.za

https://doi.org/10.18280/acsm.490503

Received: 20 June 2025
Revised: 12 August 2025
Accepted: 19 August 2025
Available online: 31 October 2025

Keywords:
oil-water separation, quartz material, hydrophobic nanoparticles, wettability, surface morphology, SEM, oil rejection efficiency, nanoparticle coating, wastewater treatment

ABSTRACT

The growing need for efficient oil–water separation technologies remains a critical challenge due to the persistence of stable emulsions in industrial wastewater. Conventional ceramic membranes are often expensive, while polymeric alternatives suffer from fouling and limited durability. This study addresses these challenges by investigating the modification of low-cost quartz particles with hydrophobic nanoparticle coatings to enhance their separation efficiency. The specific objectives were to (i) evaluate the influence of sequential nanoparticle coatings (one to four layers) on surface morphology and wettability, and (ii) develop mathematical models to quantify oil rejection efficiency and nanoparticle distribution. Experimental results revealed that a single coating produced the most uniform nanoparticle layer, achieving a significant reduction in oil and grease concentration in the permeate (29.3 mg/L). Additional coatings led to clustering and surface irregularities, which negatively impacted performance. The findings demonstrate the potential of optimized quartz-based materials as scalable and environmentally sustainable solutions for oily wastewater treatment.

1. INTRODUCTION

Industrial processes generate large volumes of oily wastewater containing stable oil-in-water emulsions that are challenging to separate. If inadequately treated, these emulsified effluents can contaminate water resources, harm aquatic ecosystems, and pose serious public health risks [1-3]. Membrane filtration is a widely used technology for oil–water separation due to its high effluent quality and energy efficiency. However, conventional membranes face significant limitations: polymeric membranes are prone to severe fouling by oil droplets (leading to flux decline and frequent cleanings), whereas ceramic membranes offer better fouling resistance but are expensive to manufacture and mechanically brittle [4-6]. This trade-off between cost and durability has motivated the search for alternative low-cost, high-performance materials for oily wastewater treatment [7-9].

Quartz has emerged as a promising candidate in this context, owing to its abundance, low cost, and chemical stability. Quartz (crystalline SiO_2) is one of the most ubiquitous minerals and can withstand harsh water treatment conditions without significant degradation [10]. Prior studies have explored sintered quartz sand membranes as a potential replacement for conventional membranes. For example, Fan et al. [11] achieved over 97% oil rejection using a quartz sand membrane with ~270 nm pores, by adding a sintering agent to improve porosity and strength. Similarly, Xiang et al. [12] reported that sintering quartz at 1000°C produced ultrafine ~16 nm pores (with high compressive strength ~31 MPa) and yielded a maximum oil removal of ~71%. These results demonstrate the viability of quartz-based filters, but the fabrication required high temperatures and careful control of pore structure. More importantly, most existing quartz membrane studies have focused on optimizing mechanical and structural properties (e.g. pore size, strength) rather than tuning surface chemistry for improved separation. Although quartz is naturally hydrophilic – its silanol-rich surface tends to attract water and repel oils–this intrinsic wettability has generally been viewed as a benefit for fouling resistance rather than actively leveraged for enhancing oil capture [13-15]. As a consequence, there is a clear research gap in understanding how modifying the quartz surface characteristics could further improve oil–water separation performance.

Surface properties are known to play a pivotal role in oil–water separation mechanisms. In general, two wettability-based strategies can be employed: (i) hydrophilic/oleophobic surfaces, which favour water wetting and form a water film that resists oil adhesion, and (ii) hydrophobic/oleophilic surfaces, which repel water while readily attracting and capturing oil. The former strategy has been used to mitigate fouling – for instance, coating membranes with hydrophilic nanomaterials (SiO_2, Al_2O_3, TiO_2, etc.) can create superhydrophilic, underwater oleophobic surfaces that inhibit oil deposition [16-18]. In contrast, the latter strategy (hydrophobic/oleophilic) is advantageous for directly removing oil from water: a material that strongly repels water but strongly attracts oil can selectively capture oil droplets and let water pass through. In fact, an ideal oil-scavenging filter is one that is superhydrophobic (water contact angle >150°) and superoleophilic, ensuring that oil is absorbed or coalesced by the material while water is excluded. Previous studies have

shown that rough, low-surface-energy coatings can achieve this effect. For example, Kumari et al. [19] functionalized silica wool to be extremely water-repellent and oleophilic, enabling it to absorb oils from water with high efficiency (oil was taken up into the material's pores while water was cleanly repelled). Likewise, a recent study by Hou et al. [20] produced micro/nano-structured quartz sand with a water contact angle of ~154° (superhydrophobic) and near-zero oil contact angle, which exhibited excellent oil removal efficiency. These works underscore the significance of surface wettability: by tailoring a quartz-based medium to be hydrophobic, one can impart it with oleophilic characteristics that greatly enhance oil capture from emulsions.

Hydrophobic nanoparticle coatings offer a practical route to modify quartz surfaces for this purpose. Depositing a layer of hydrophobic nanoparticles onto quartz can lower the surface energy (through hydrophobic functional groups) and increase the surface roughness at the micro/nanoscale [21-23]. This combination is known to produce a Cassie–Baxter state where water contacts only the tips of surface asperities and air pockets occupy the rest, causing water to bead up and roll off. The nanoparticles' hydrophobic chemistry (e.g. siloxane or fluorinated alkyl groups) inherently repels water molecules, while the nanoscale texture amplifies this repellence by trapping air beneath droplets [24]. At the same time, such hydrophobic coatings are typically oleophilic, meaning that nonpolar oil fluids will spread over and adhere to the coated surface. In a packed bed of quartz grains, a uniform hydrophobic nanoparticle coating on each grain would thus create an interconnected superhydrophobic network that resists water intrusion but readily adsorbs oil. As oily water flows through, the coated quartz should selectively capture and coalesce oil droplets (which stick to the hydrophobic surface), allowing purified water to permeate. This concept of surface-engineered quartz could combine the low cost and robustness of quartz with the selectivity of special wettability, potentially yielding an efficient and reusable oil–water separation medium.

Despite this compelling rationale, the optimal way to apply hydrophobic nanoparticle coatings on quartz remains uncertain. An insufficient coating may fail to render the surface fully hydrophobic, whereas an excessive coating could cause nanoparticle agglomeration, surface blocking, or even a loss of the superhydrophobic effect due to wettability transitions. In other words, more coating is not necessarily better – beyond a certain point, additional nanoparticle layers might create surface defects (e.g. clusters, cracks) that undermine the material's oil-repellent behaviour. For instance, overly rough or thick coatings can force a surface into the fully wetted Wenzel state, nullifying the lotus-effect of a superhydrophobic surface. To date, however, no systematic study has been reported on how sequential hydrophobic nanoparticle layers affect the morphology and performance of quartz-based separators. This knowledge gap has hindered the informed design of coated quartz filters for oil–water separation [25-27].

The present study addresses this gap by investigating the impact of hydrophobic nanoparticle coatings on quartz particles for enhanced oil–water separation. In particular, we modified dry-graded quartz sand (0.8–1.8 mm particles) with one to four sequential layers of hydrophobic nanoparticles and evaluated the resulting changes in surface characteristics and separation efficiency. The novelty of this work lies in the systematic layering of nanoparticles on a naturally low-cost mineral substrate, as well as the integration of mathematical modelling to interpret the experimental results. The specific objectives were to: (i) evaluate how increasing the number of nanoparticle coating layers (from 1 through 4) influences the quartz surface morphology, wettability, and oil rejection capability; and (ii) develop quantitative models to predict key performance metrics (oil rejection efficiency, permeability, and nanoparticle distribution uniformity) based on coating properties. We hypothesized that a single, well-distributed hydrophobic coating would create an optimal superhydrophobic surface on quartz, maximizing oil capture and minimizing fouling. By contrast, additional coatings were expected to produce diminishing or negative returns, as nanoparticle overloading could introduce irregularities and pore constrictions that impair separation performance. In the following sections, we demonstrate that an optimized one-layer nanocoating indeed provides the best oil–water separation results, and we discuss the fundamental implications of these findings for designing scalable, environmentally sustainable quartz-based filtration media.

2. MATERIALS AND METHODS

2.1 Quartz material selection and justification

Dry-graded silica quartz particles (SiO_2 98%, Fe_2O_3 0.18%, particle size 0.8–1.8 mm) were selected for this study as indicated in Figure 1. Quartz was chosen due to its abundance, low cost, chemical inertness, and mechanical durability under harsh operating conditions, making it an attractive low-cost alternative to conventional ceramic membranes. The selected particle size range (0.8–1.8 mm) provided an optimal balance between permeability and surface area for effective interaction with hydrophobic nanoparticles, thereby enhancing oil–water separation efficiency. This size also mimics granular filtration media, ensuring adequate packing density without excessive flow resistance.

2.1.1 Crushing and preparation of quartz particles

The quartz particles were obtained by mechanical crushing of bulk quartz using a laboratory jaw crusher. The crushed material was then sieved to isolate the 0.8–1.8 mm fraction. This controlled crushing and sieving ensured a uniform particle size distribution while preserving sufficient surface roughness to promote nanoparticle adhesion. Following size classification, the particles were thoroughly washed with a descaling chemical solution to remove surface impurities (e.g., clay, dust, and mineral residues) and rinsed with deionized water. The cleaned quartz was dried at 25°C for 24 hours to prepare for coating.

2.1.2 Nanoparticle coating procedure and rationale

Hydrophobic nanoparticles were applied to the quartz particles using a high-pressure spray gun. To investigate the effect of coating thickness and surface morphology on oil–water separation, quartz samples were sequentially coated with one to four layers of nanoparticles. The rationale was that:

- A single coating was expected to provide uniform nanoparticle coverage, creating an optimal hydrophobic/oleophilic surface for oil capture.
- Additional coatings (2–4 layers) were included to study the impact of increased nanoparticle density, potential

clustering, and surface roughness on wettability and oil rejection.

This systematic layering approach enabled evaluation of whether performance improvements plateau or decline with successive coatings, thereby identifying the optimal coating condition.

Coated particles were categorized into four groups: raw (unmodified), washed (cleaned), and coated with one to four nanoparticle layers. Each group was subjected to Scanning Electron Microscopy (SEM) to analyse surface morphology and nanoparticle distribution. Wettability tests and oil–water separation experiments were then performed to quantify performance differences among the samples.

Figure 1. Crushed quartz particles

After crushing, the quartz material was thoroughly cleaned using a descaling chemical to eliminate surface impurities and contaminants prior to coating. The cleaned quartz was then air-dried at room temperature (25 °C) for 24 hours. Once dry, the material was spread in a thin, even layer on a flat surface. A high-pressure spray gun was employed to apply hydrophobic nanoparticles to the quartz particles, aiming to enhance surface wettability. Coatings were applied sequentially, ranging from one to four layers, to evaluate their performance in oil-water separation [28].

To ensure uniform coating, the spray gun nozzle was positioned at a 90-degree angle, maintaining a 5 mm distance from the particle surface. After coating, the quartz particles were prepared for analysis using Scanning Electron Microscopy (SEM) to examine surface morphology, as illustrated in Figure 2. For a comprehensive comparison of surface wettability, the samples were categorized into four groups: raw, washed, and coated (with one to four layers of nanoparticles).

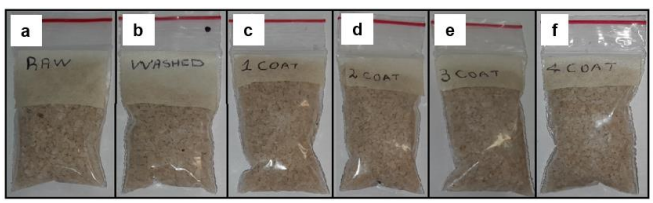

Figure 2. Quartz samples for SEM characterization: (a) Raw; (b) Washed; (c) First coating; (d) Second coating; (e) Third coating; (f) Fourth coating

2.2 Oil/water separation using quartz martial

Dry-graded silica particles (SiO_2 98%, Fe_2O_3 0.18%, particle size 0.8–1.8 mm) were utilized to investigate the quality of permeate during oil-water separation. The study employed the gravitational bed gravity-accelerated technique, as illustrated in Figure 3, to ensure a separation process free from mechanical or electrical influence. Diesel in water was used to simulate industrial oily wastewater in the experiments.

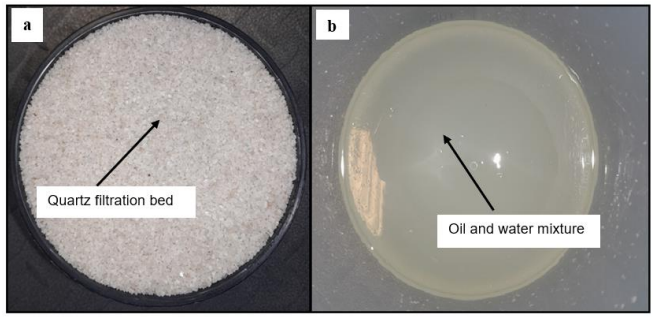

Figure 3. Quartz material for oil–water separation: (a) Quartz filtration bed; (b) Oil–water mixture

2.3 Mathematical models developed to analyze quartz material performance

The mathematical models were developed to analyze the performance of quartz materials in oil-water separation.

Eq. (1) indicates the Oil Rejection Efficiency (ORE), this model measures the quartz material's ability to reduce oil content after treatment, where $C_{initial}$ is oil and grease concentration in the feed water (mg/L) and C_{final} represents the Oil and grease concentration in the treated water (mg/L).

$$ORE(\%) = \frac{C_{initial} - C_{final}}{C_{initial}} \times 100 \quad (1)$$

Eq. (2) represents the Surface Wettability Contribution (SWC), this model evaluates the contribution of surface wettability to the oil rejection process, accounting for the number of coatings, where n is the number of hydrophobic nanoparticle coatings applied to the quartz material.

$$SWC = \frac{ORE(\%)}{n} \quad (2)$$

Eq. (3) indicates the Separation Performance Index (SPI), the SPI assesses the material's efficiency in separating water from the oil-water mixture, incorporating permeate volume and feed concentration. Where $V_{Clean\ water}$ is the Volume of water separated (L) and $V_{total\ feed}$ is the total volume of the oil-water feed (L).

$$SPI = \frac{V_{Clean\ water}}{V_{total\ feed}} \times OER \quad (3)$$

Eq. (4) shows the Nanoparticle Coverage Consistency (NCC), to assess the uniformity of nanoparticle coating on the quartz surface, this equation was developed based on SEM image data. Where σ_s is standard deviation of inter-particle distances (μm) and μ_s is mean inter-particle distance (μm).

$$NCC = 1 - \frac{\sigma_s}{\mu_s} \quad (4)$$

Eq. (5) shows the Surface Morphology Factor (SMF), where surface roughness plays a role in oil separation. The SMF quantifies the relationship between roughness and effective surface area, where A_{actual} is the measured surface area, considering roughness and A_{flat} indicates the projected flat surface area.

$$SMF = \frac{A_{actual}}{A_{flat}} \quad (5)$$

Eq. (6) represents the Oil Removal Capacity (ORC), this model calculates the amount of oil removed by the material per unit mass or volume of quartz, where M_{quartz} is the mass of quartz material used (g).

$$ORC = \frac{C_{initial} - C_{final}}{M_{quartz}} \quad (6)$$

Using these models, the efficiency and performance metrics for each coating stage (raw, washed, first to fourth coatings) can be calculated. For example:

- **ORE and SWC** help determine the effectiveness of each coating.
- **NCC and SMF** evaluate nanoparticle orientation and surface morphology from SEM data.
- **SPI and ORC** provide insights into separation efficiency and the material's oil removal capacity.

3. RESULTS AND DISCUSSIONS

The SEM was used to investigate the surface morphology of quartz particles and the gravitational bed gravity-accelerated technique was used to validate the microscopic results. The permeate quality was assessed using the oil and grease analysis to test the water quality after oil and water separation.

3.1 SEM analysis

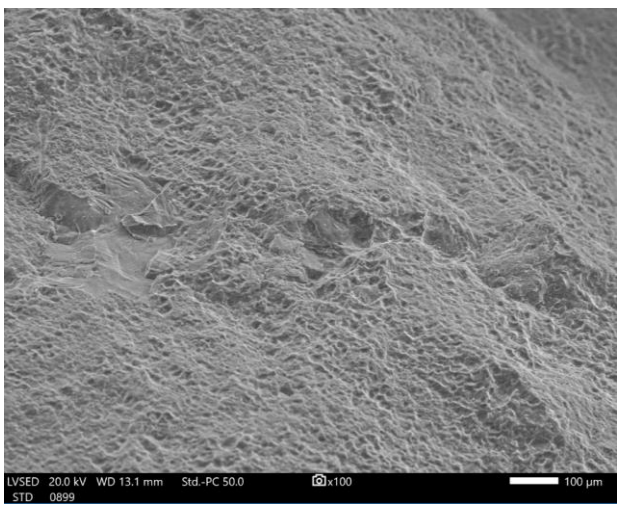

Figure 4. SEM image of raw quartz material showing untreated surface morphology

Figures 4-9 below present the Scanning Electron Microscopy (SEM) results obtained during the analysis of quartz material. The images include the raw quartz (Figure 4), the quartz material after the washing process (Figure 5), and the surfaces coated with hydrophobic nanoparticles, progressing from the first coating (Figure 6) to the fourth coating (Figure 9). These results illustrate the changes in surface morphology at each stage of preparation and coating.

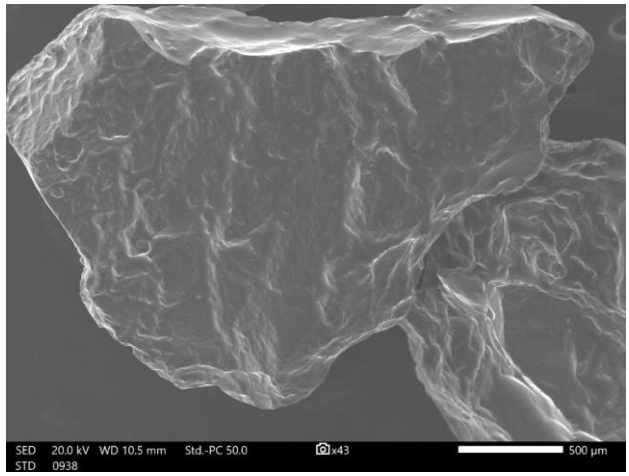

Figure 5. SEM image of washed quartz material showing cleaned surface morphology

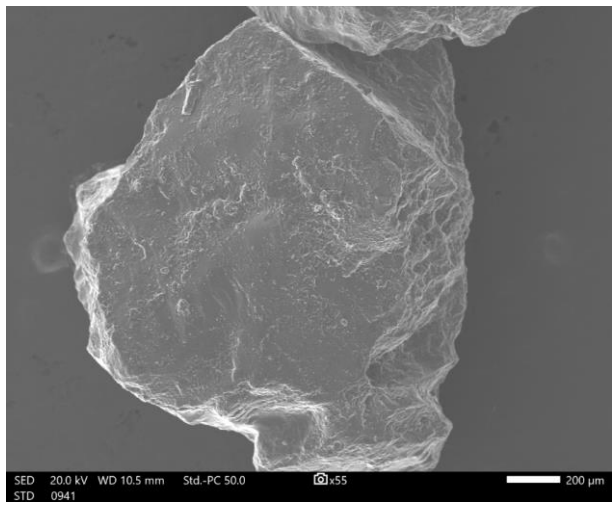

Figure 6. SEM image of quartz material after first nanoparticle coating showing initial surface coverage

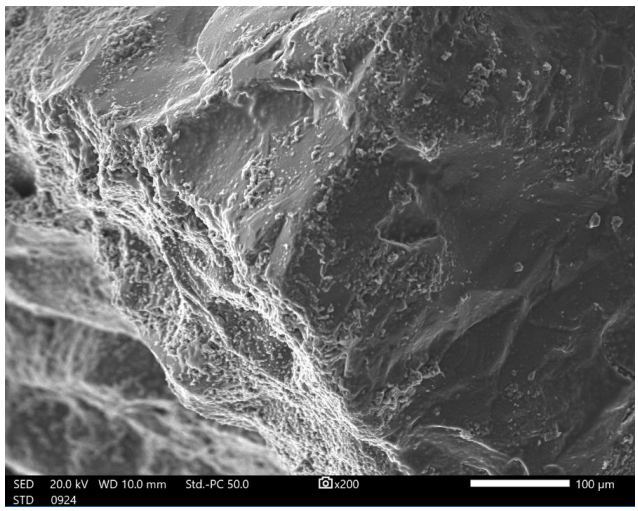

Figure 7. SEM image of quartz material after second nanoparticle coating showing increased surface coverage

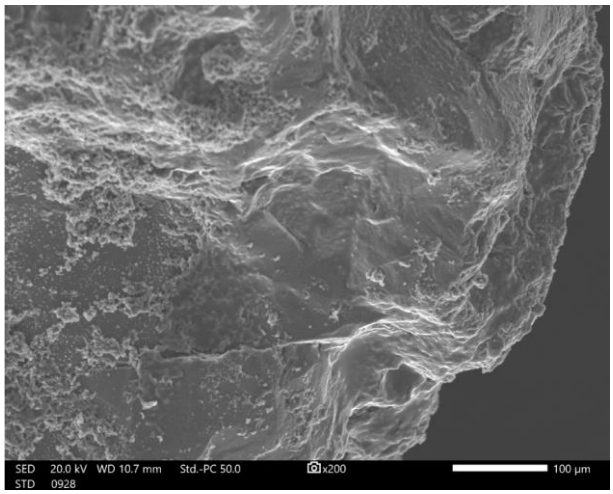

Figure 8. SEM image of quartz material after the third nanoparticle coating showing progressive layer buildup

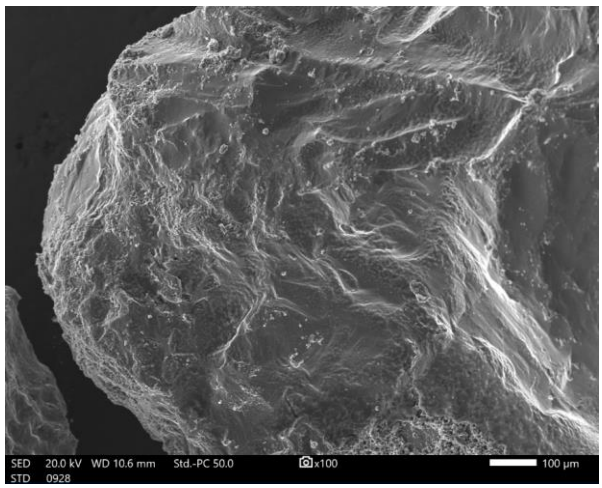

Figure 9. SEM image of quartz material after fourth nanoparticle coating showing enhanced and uniform surface coverage

Figure 4 shows the SEM image of the raw, unmodified quartz particle surface prior to any treatment. The raw quartz exhibits a rough, uneven topology with numerous irregular features and inherent impurities or contaminants scattered across the surface. These may include fine clay, dust, or mineral residues attached to the quartz [29, 30]. The surface roughness is inconsistent and uncontrolled, characterized by jagged protrusions and crevices of various sizes. Without any coating, the quartz's native silica surface likely presents hydrophilic silanol groups, meaning the surface chemistry is inherently high-surface-energy (hydrophilic). Thus, water would spread more easily on such a surface, and oil droplets could also foul or adhere due to the contaminants. The lack of an intentional nano-scale texture or low-energy coating leaves the raw quartz with minimal water-repellent properties. Any surface irregularities present are not engineered for wettability control but rather are random defects that can trap water or oil [31-33].

Since no nanoparticles are applied at this stage, the concept of "distribution" doesn't apply yet; instead, we focus on the distribution of natural impurities. In the raw state, foreign particles and contamination are unevenly distributed on the quartz, as evidenced by dark or light spots in the SEM image. These contaminants can create localized wetting sites that further reduce the quartz's ability to repel water. In effect, the raw quartz surface is highly wettable by water (hydrophilic) and lacks any hydrophobic behaviour. This is evidenced by extremely poor oil-water separation performance: in oil-and-grease tests, water filtered through raw quartz contained very high oil concentrations (~1859.8 mg/L), indicating that most of the oil was not captured or separated. Such high oil content in the permeate underscores that the untreated, rough surface cannot repel water or oil effectively – oil passes through freely with the water because the surface has no hydrophobic rejection capability. The presence of surface impurities likely exacerbates this, as they can destabilize emulsions or provide pathways for oil to traverse. In summary, Figure 4's raw quartz SEM reveals a coarse, dirty surface that correlates with poor separation efficiency due to lack of hydrophobicity. This baseline highlights the need for surface modification to improve wettability for oil-water separation.

Figure 5 displays the SEM image after the quartz particle has been washed to remove impurities. Compared to Figure 4, the surface appears markedly cleaner and somewhat smoother. Many of the particulates and residues visible in the raw quartz image are gone, resulting in a more uniform base texture. The underlying quartz surface features (grain boundaries, micro-roughness of the mineral itself) are now exposed without the masking layer of dirt. The washing process does not fundamentally change the quartz's natural roughness on the microscale, but it eliminates foreign debris, yielding a more uniform roughness profile across the surface. We observe that some surface asperities remain (since the quartz itself is not polished), but these are intrinsic to the quartz morphology rather than random contaminants. Overall, the washed quartz shows a consistent topography with reduced small-scale heterogeneity. This improved cleanliness is important for subsequent nanoparticle coating, as a clean, uniform substrate promotes better adhesion and distribution of the coating. In essence, Figure 5 confirms that the washing step successfully prepares the quartz by producing a smoother and contaminant-free surface suitable for coating.

Despite the removal of impurities, the washed quartz surface is still composed of bare silica and thus remains hydrophilic. The SEM does not show any nanoparticles yet (since coating hasn't begun), but the more uniform surface means there are fewer unpredictable wetting sites due to dirt. This yields a slight improvement in oil-water separation compared to raw quartz, but the effect is marginal. Oil-and-grease analysis shows the washed quartz achieved a residual oil concentration of ~1583.7 mg/L, a modest reduction from the raw's 1859.8 mg/L. This ~15% improvement suggests that removing contaminants helps a little – likely because some extremely wettable or oil-attractive sites were eliminated – but by itself is insufficient for effective separation. The washed surface still lacks low-surface-energy coating, so water can wet it and oil can still pass through. The SEM observation of a cleaner surface correlates with this small performance change: cleanliness alone improved uniformity but did not impart hydrophobicity. Thus, while Figure 5 indicates progress in surface preparation (essential for coating adhesion), the quartz at this stage is still poorly suited to repel water or capture oil, as reflected by the still-high permeate oil levels. In practical terms, the washing step is necessary but not sufficient – it paves the way for the critical addition of hydrophobic nanoparticles in subsequent steps, which we expect to dramatically alter both the SEM appearance and the wettability.

Figure 6 provides the SEM image of the quartz surface after applying the first hydrophobic nanoparticle coating. The difference from Figure 5 is striking – the once-bare quartz surface is now uniformly covered with a layer of nanoparticles. These nanoparticles appear as a fine granular texture blanketing the entire surface. The distribution is relatively even and monodisperse, meaning the particles are spread out without large agglomerates or bare patches. We observe that individual nanoparticles (likely on the order of tens of nanometres to a few hundred nanometres in size) are each distinguishable and spaced in a consistent manner. The inter-particle separation distances are small and fairly uniform, creating a coherent coating. Importantly, there is minimal clustering visible – the particles do not form big "islands" or piles on the surface at this stage. This indicates successful deposition of a single layer where particles attach primarily to the quartz and to each other in a controlled fashion.

The resulting coated surface has a controlled nano-scale roughness: the nanoparticles themselves introduce texture, but because they are evenly distributed, the roughness is hierarchical and homogeneous rather than random. Such a surface structure is known to be beneficial for hydrophobicity – it resembles a lotus-leaf-like texture where tiny protrusions cover the surface [34-36]. The SEM suggests this first coating achieves an optimal roughness balance: the surface is no longer smooth, but it's not excessively jagged either; it has a fine carpet of nano asperities. This kind of uniform nano-rough surface, combined with the hydrophobic material of the nanoparticles, is expected to yield superhydrophobic behaviour. Indeed, the even coverage maximizes the exposure of low-surface-energy material (assuming the nanoparticles or their coating are hydrophobic, such as silanized silica) to any contacting liquid.

The first coating dramatically transforms the surface wettability. With the uniform layer of hydrophobic nanoparticles, the quartz now presents a low-energy, water-repellent interface to any fluid. Water droplets contacting this surface would encounter a forest of hydrophobic nanoparticle tops, likely causing the droplet to sit in a Cassie–Baxter state (resting on the tips of particles with air trapped underneath) [37]. This results in high contact angles (water forms nearly spherical droplets) and very low water adhesion – droplets would roll off easily, as qualitatively noted in the study. In practical terms, this means the surface strongly resists wetting by water while favouring oil (oleophilicity), which is ideal for oil-water separation: water is repelled and can flow off or be collected as clean permeate, whereas oil, being non-polar, can be preferentially absorbed or retained by the hydrophobic surface [38].

The oil-rejection performance after one coating is evidence of this optimal wettability – the oil and grease content in the water permeate plummets to 29.3 mg/L, a drastic reduction compared to the uncoated and washed cases. This ~98% reduction in residual oil (relative to raw) indicates that the first coated quartz effectively captures or repels oil, allowing mostly clean water through. Such performance is on par with what one would expect from a superhydrophobic filter material, and it aligns with literature where a single hydrophobic nanoparticle layer can create a high-performance oil-water filter. The key is that the first coating creates a continuous, defect-free hydrophobic surface. The SEM's lack of large bare spots or big clusters means there are no hydrophilic "weak spots" where water could penetrate or wet the surface. The roughness introduced is just enough to amplify hydrophobicity (as roughness amplifies the intrinsic water-repellent nature of the coating) without causing water to get pinned in crevices. In summary, Figure 6 reveals that one nanoparticle coating yields a uniformly nanostructured, hydrophobic surface with an excellent balance of roughness and coverage, which translates to the best oil-water separation efficiency observed among all stages.

Figure 7 shows the quartz surface after a second layer of hydrophobic nanoparticles has been added on top of the first. At first glance, the surface still appears coated, but a closer look at the SEM reveals subtle but important changes in morphology. With the additional coating, the surface roughness increases – the nanoparticles from the second layer add another tier of texture. We can see that some areas have thicker clusters or aggregates forming: unlike the first coat's uniformly peppered appearance, the second coat introduces regions where nanoparticles have piled up slightly, creating small cluster "islands." In other areas, the coverage remains fairly even. Overall, the coating is still present everywhere (no completely bare patches), but the uniformity is slightly reduced. The inter-particle distance on average becomes narrower because new nanoparticles occupy some of the gaps that existed after the first coat – essentially, the surface is moving toward a more closely packed state [39, 40]. However, because the second coat cannot perfectly evenly distribute (some particles preferentially nucleate on existing ones), we start to see incipient clustering. These clusters might look like tiny bumps or agglomerates in the SEM image, indicating where multiple nanoparticles have stacked or sintered together. The surface roughness is now higher in those clustered regions (since the clusters protrude more), giving the surface a slightly more irregular topography compared to the single layer. In summary, the second coating results in increased nanoparticle coverage (denser packing) but at the cost of introducing minor irregularities in the coating layer.

With a second layer, the surface is still hydrophobic overall – after all, it's still coated in hydrophobic nanoparticles – and the increased roughness can even further enhance water repellence to a point. However, the loss of perfect uniformity means the wettability is not as consistently optimal across the entire surface [41, 42]. Most of the surface remains extremely hydrophobic, but where slight clustering has occurred, there could be micro-scale valleys or texture that allow water to anchor more than on the perfectly uniform first coat. In effect, the surface has a mix of very hydrophobic regions and some that are slightly less so due to uneven texture. The oil-water separation performance after two coatings reflects a decline from the optimum: the oil content in permeate rises to 547.4 mg/L. This is a notable increase compared to the mere 29.3 mg/L after one coat, though 547 mg/L is still much lower than the untreated cases. The performance drop (~half a gram of oil per litter vs ~0.03 g/L earlier) suggests that the second coating, while still providing a hydrophobic barrier, has compromised the efficiency.

Likely, the slight clustering caused some oil to bypass or some water to carry oil through. Another possibility is that by adding more particles, the surface's pore structure or flow pathways changed – maybe creating channels where oil could slip through more easily. In terms of wettability, we might infer that contact angles are still high on average, but contact angle hysteresis (the difference between advancing and receding angles) might increase due to surface heterogeneity. In plainer terms, water droplets might still bead up, but some pinning could occur at the clustered spots. The SEM evidence

of emerging clusters aligns with this performance: clustering disrupts the previously uniform hydrophobic network, causing uneven wettability across the surface. Yet, because the majority of the surface remains coated and hydrophobic, the second-coated quartz still outperforms raw or washed quartz by a wide margin. The similarity between the first and second coating stages is that both are hydrophobic and rough, enabling relatively good separation compared to no coating; the difference is that the second coating has entered a regime of diminishing returns, where adding more nanoparticles no longer improves, and indeed harms, the separation efficiency. Figure 7 thus illustrates that while adding a second nanoparticle layer increases surface roughness and coating density, it can introduce minor flaws (clusters) that start to undercut the ideal superhydrophobic behaviour achieved with one layer.

Figure 8 presents the quartz surface after a third consecutive nanoparticle coating has been applied. By this stage, the SEM image shows the surface has become considerably more irregular. The accumulation of three layers of nanoparticles leads to a significant increase in surface roughness and prominent nanoparticle clustering. In the image, one can observe large, agglomerated features – these could be described as "cauliflower-like" clusters where many nanoparticles have clumped together. There are fewer areas of exposed, individual nanoparticle texture; instead, the surface is dominated by these clusters and lumps [43]. This indicates that the surface is nearing saturation coverage: most of the available surface sites were occupied by the first two coats, and the third-coat nanoparticles end up attaching onto existing particles rather than finding new bare quartz to adhere to.

The result is stacking of nanoparticles in a somewhat uncontrolled manner. Some regions might have triple-layer thickness of particles, while others might have double or single layers, causing a highly uneven coating thickness across the surface. The inter-particle separation distance, on average, decreases further – effectively, the particles (and clusters thereof) are now so close that the concept of distinct separation starts to blur. In some spots, the coating may have even formed a quasi-continuous nanoparticle film. This heavy texture gives the surface a very rough, bumpy profile, with peaks (at cluster tops) and valleys (in between clusters). Such morphology is quite different from the uniformly rough first coating: it lacks homogeneity. Additionally, the orientation and arrangement of nanoparticles become less controlled – particles in the third layer might sit at various angles or partially embed into lower layers, creating complex geometries. In summary, the third coating oversaturates the surface with nanoparticles, leading to pronounced roughness and irregular, cluster-dominated morphology [44].

Wettability Degradation: Interestingly, adding this third layer – one might expect it to further increase hydrophobicity by adding more roughness – actually results in a decrease in effective hydrophobic performance. The SEM's evidence of clustering and lost uniformity explains why: the surface now likely has regions where water can penetrate or become trapped (the "valleys" between clusters can retain liquid, defeating the lotus effect). The formerly optimal nano-roughness is overshot, potentially transitioning some areas from a Cassie-Baxter state (droplets resting on particles with air underneath) to a Wenzel state (water penetrating and wetting the rough surface). Moreover, some parts of the surface might not be fully coated if clusters drew nanoparticles away, leading to minor exposed hydrophilic quartz patches. These effects would make the surface overall less water-repellent than the first or even second coat. The oil-water separation results are dramatically worse: after three coatings, the oil content in the effluent water spikes to about 27,177 mg/L. This extremely high value (two orders of magnitude higher than even the raw quartz case) indicates near-total failure of separation at the third coating stage. Essentially, the quartz with three coatings not only didn't improve separation – it made it so poor that the water coming through had an even higher concentration of oil than the original feed (this suggests emulsified oil might have been *stabilized* or carried by the altered surface).

While that result seems counter-intuitive, it could be that the rough, clustered surface tends to trap oil within its crevices and then re-entrain it into the water, or possibly the clusters create channels that preferentially allow oil to pass. Another possibility is that the dense coating significantly reduced permeability or changed flow patterns, causing a high local concentration of oil in fewer channels. Regardless, from a wettability standpoint, the third coating clearly introduces adverse effects: excessive roughness and clustering create localized wetting and fouling spots, reducing the overall hydrophobic effectiveness. In plainer terms, water can no longer roll off the surface cleanly; instead, it contacts more of the surface and can pick up oil that has accumulated on the rough clusters [45]. The drastic rise in oil content (to tens of grams per litter) underscores that the material has become ineffective as a filter, likely saturating with oil and letting oil through. Figure 8, therefore, highlights a critical turning point: whereas one or two coatings were beneficial, a third coating over-saturates the surface with nanoparticles, leading to irregular morphology that severely diminishes oil-water separation efficiency. It emphasizes that more coating is not always better – there is an optimal coating thickness, beyond which performance degrades.

Figure 9 shows the SEM image after the fourth hydrophobic nanoparticle coating, representing the most extreme case of coating in this series. By this stage, the quartz surface is densely packed and heavily encrusted with nanoparticles, to the point of oversaturation. The SEM likely reveals a surface almost entirely covered by thick clusters; any semblance of the original quartz topology is buried under multi-layered nanoparticle agglomerates. Some regions might exhibit flaky or chunky deposits where the nanoparticles have aggregated massively. Because additional particles from the fourth coat have nowhere else to attach, they pile onto existing cluster peaks, making those clusters even larger [46]. Paradoxically, some other regions might receive comparatively fewer new particles (if the majority stick to certain nucleation sites), meaning the coating is highly uneven – oversaturated in some spots and possibly under-saturated in others. This non-uniform deposition results in a patchwork of heavily coated "mountains" adjacent to somewhat thinner "valleys." The inter-particle separation is minimal; in fact, many particles are likely touching or fusing together in the clusters. At this level of coverage, the surface roughness is extremely high at the cluster scale, but the microscopic texture might effectively smooth out (imagine filling a surface with so many particles that it becomes one continuous mass of coating with a relatively smoother outer contour on the large scale, albeit made of irregular lumps) [47]. In short, the fourth coating creates a severely irregular, bumpy surface with large cluster formations and no semblance of the fine, distributed roughness that was seen after the first coat. If chunks of the coating are

unstable, they could even break loose or shift, further degrading the structural integrity of the coating.

The wettability and oil-water separation performance with four coatings are the worst of all stages [48, 49]. The surface, being fully covered in hydrophobic material, is still hydrophobic in a chemical sense; however, its physical texture is so rough and erratic that it no longer effectively repels water uniformly. Water may penetrate the deep recesses between large clusters, becoming partially trapped, and thus wets the surface to a greater extent. Also, any slight undercoated regions can act as wetting hotspots, immediately compromising the overall hydrophobicity. The result is a mixed wetting regime where the benefits of hydrophobic chemistry are negated by the flawed morphology. The oil and grease analysis shows an extremely high oil concentration (~73,439.7 mg/L) in the water after filtration with the four-times-coated quartz. This is an astonishingly poor result – effectively, the water is heavily oil-laden, far worse than even untreated water. Such a high value suggests that the filter might have released previously captured oil, or that the structure caused almost all oil to pass through, perhaps even concentrating it.

We can interpret that by the fourth coat, the quartz particle bed could be so clogged with hydrophobic material and oil that when water flows, it sweeps oil out with it, leading to extremely oil-rich effluent. In terms of wettability, the fourth-coated surface [50] likely has lost the lotus effect entirely; any water contacting it can wet certain parts and pick up oil from the saturated clusters. Additionally, flow channels might form between unevenly coated regions, offering oil an easy path. The SEM description notes that the surface morphology "no longer supports optimal hydrophobicity"– essentially, the surface fails to function as a repellent interface. The fourth coating demonstrates diminishing returns to the extreme: not only is there no benefit to adding more nanoparticles beyond the first layer, but by the fourth layer the performance is severely worse than no coating at all. This underscores that an oversaturated, overly rough surface is detrimental. The similarity between the third and fourth coatings is that both show heavy clustering and poor performance, but the fourth is an even more exaggerated case. Figure 9's outcome solidifies the trend that excessive nanoparticle layering is counterproductive, as it creates a chaotic surface that undermines the very goal of enhancing oil-water separation.

3.1.1 Oil and grease analysis

The oil and grease analysis was performed to assess the quality of permeate (water) obtained after the oil/water separation process. This evaluation aimed to determine the effectiveness of quartz material in separating oil/water emulsions. The findings from the analysis are summarized in Table 1, highlighting the performance of the quartz material under different conditions.

The findings revealed that the best results were observed with the first coating, where the hydrophobic nanoparticles were evenly distributed, ensuring optimal wettability and efficient separation. While, additional coatings introduced irregularities, clustering, and excessive roughness, which compromised the separation efficiency and led to significantly higher oil content in the permeate.

3.1.2 Comparison of oil and grease analysis with SEM findings

The findings from Table 1 and the SEM analysis converge to highlight the exceptional performance of the first coating. The uniform nanoparticle distribution and balanced surface properties observed in the SEM analysis directly justify the low oil and grease content (29.3 mg/L) achieved in Table 1. Subsequent coatings degrade performance due to increased roughness, clustering, and loss of uniformity, underscoring the importance of optimizing the coating process for practical applications. Table 2 shows the comparison of oil and grease analysis with SEM findings.

The analysis of Table 2 highlights the critical impact of surface morphology and nanoparticle distribution on the quartz material's ability to separate oil from water. The raw and washed quartz materials demonstrated poor separation efficiency due to the absence of hydrophobic properties, as indicated by high oil and grease content (1859.8 mg/L and 1583.7 mg/L, respectively). Washing improved surface cleanliness but did not significantly enhance wettability.

The first coating of hydrophobic nanoparticles showed exceptional performance, reducing oil and grease content to 29.3 mg/L. This was attributed to the uniform nanoparticle distribution observed in the SEM analysis, which created an optimal balance of surface roughness and smoothness. This configuration enhanced wettability, allowing efficient oil rejection and water permeation.

Subsequent coatings (second to fourth) led to a decline in separation efficiency, with oil and grease content increasing dramatically. The SEM analysis revealed that additional coatings introduced clustering, excessive surface roughness, and irregular morphology, disrupting the uniform wettability necessary for effective oil-water separation. The oversaturation of nanoparticles in the fourth coating resulted in severe inefficiencies, with oil and grease content rising to 73439.7 mg/L.

Table 1. Impact of nanoparticle coatings on quartz material

Quartz Material	Oil and Grease (mg/L)	Impact of Nanoparticles
Raw	1859.8	No treatment; high oil content due to lack of hydrophobic properties.
Washed	1583.7	Removal of surface impurities slightly reduces oil content but lacks hydrophobicity for effective separation.
First coating	29.3	Achieves the most efficient oil-water separation. Uniformly distributed nanoparticles enhance wettability, significantly reducing oil content in permeate.
Second coating	547.4	Slightly less effective; increased roughness and nanoparticle clustering reduce uniform hydrophobic coverage.
Third coating	27177	Poor performance; excessive nanoparticle layering and clustering increase hydrophobic irregularities, trapping oil.
Fourth coating	73439.7	Ineffective; oversaturation of nanoparticles disrupts surface properties, causing severe inefficiencies in separation.

Table 2. Comparison of oil and grease analysis with SEM findings

Quartz Material	Oil and Grease (mg/L)	SEM Findings	Justification
Raw	1859.8	Rough, uneven surface with contaminants; no hydrophobic properties.	High oil content due to poor wettability and lack of treatment.
Washed	1583.7	Cleaner surface with reduced impurities; lacks hydrophobic properties.	Slight reduction in oil content; impurities removed but hydrophobicity still absent.
First coating	29.3	Uniform nanoparticle distribution, minimal clustering, optimal surface roughness and smoothness.	Best performance; enhanced wettability due to balanced surface morphology, allowing effective oil rejection and clean water permeation.
Second coating	547.4	Increased surface roughness, slight nanoparticle clustering, reduced uniformity.	Performance declines as clustering disrupts uniform wettability, leading to variability in oil rejection.
Third coating	27177	Significant clustering, excessive roughness, irregular surface morphology.	Inefficient separation due to excessive nanoparticle layers and clustering, which trap oil and reduce hydrophobicity.
Fourth coating	73439.7	Oversaturated surface with severe clustering and disrupted morphology.	Extremely poor performance; oversaturation causes irregularities, leading to oil retention and minimal water separation efficiency.

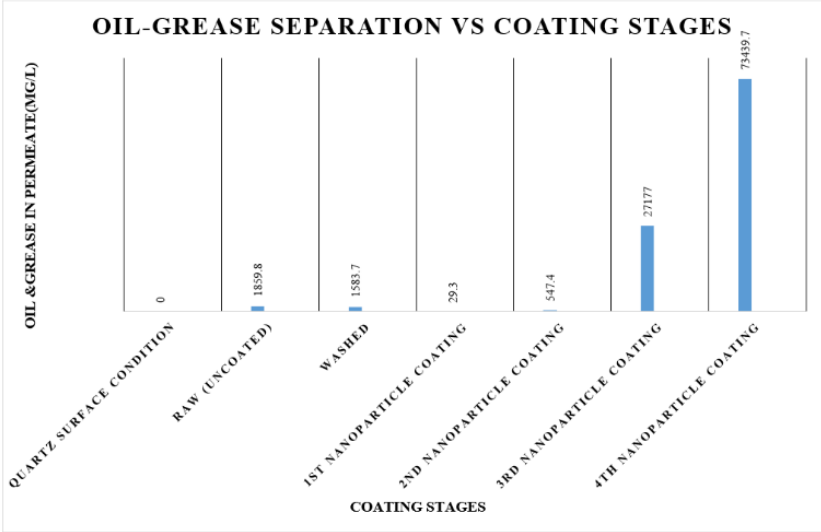

Figure 10. Oil–grease separation performance at different quartz surface conditions and nanoparticle coating stages

Overall observation, the findings underscore that a single, well-distributed coating of hydrophobic nanoparticles provides optimal separation performance, while excessive nanoparticle layering diminishes efficiency due to surface irregularities and clustering. These results emphasize the importance of optimizing coating processes for practical applications in oil-water separation technologies.

3.1.3 Comparison and overall implications

Figure 10 shows oil and grease content (log scale, mg/L) remaining in water after separation for each quartz surface condition: Raw, Washed, and with 1st through 4th nanoparticle coatings. This comparison bar chart highlights the dramatic non-linear trend in separation performance across coating stages. The first nanoparticle coating yields the lowest oil content (~29.3 mg/L), reflecting excellent separation, whereas additional coatings progressively increase the oil content in the permeate. Notably, by the third and fourth coatings, the residual oil shoots up by orders of magnitude (tens of thousands mg/L), indicating a severe decline in efficiency with over-coating. The raw and washed quartz have high oil levels (around $1.6–1.9\times10^3$ mg/L) due to lack of hydrophobicity, only modestly improved by cleaning. In contrast, the single coated quartz's superior performance is evident as a major drop on the chart, emphasizing its optimal surface morphology for oil rejection. The worsening performance with the 2nd, 3rd, and 4th coatings (blue bars climbing higher again) correlates with the increasing surface roughness and nanoparticle clustering observed in Figures 7-9. Thus, Figure 10 reinforces that one good coating is optimal, while more coatings lead to performance degradation.

To synthesize the findings from Figures 4-10, Table 3 summarizes the surface characteristics observed in SEM alongside the measured oil content in water for each stage.

The above comparisons make clear that the first nanoparticle coating provides the optimal surface for oil-water separation, balancing roughness and coverage to maximize hydrophobicity. This stage achieved a nearly continuous hydrophobic nanoparticle network on quartz, yielding superior wettability (water-repellence) which directly translated to the lowest oil content in the filtrate. By fostering a Cassie-Baxter state (water touching only the tips of hydrophobic NPs) and presenting no significant wetting defects, the single-layer coating ensures that oil droplets are largely excluded from the permeate. In contrast, subsequent coatings progressively degrade these ideal conditions. The second coat, while still relatively effective, introduced slight nanoparticle aggregation that diminished the uniform hydrophobic coverage, explaining its higher residual oil. The third and fourth coats exacerbated this, creating extensive clustering and possibly clogging effects that resulted in trapped oil and loss of

superhydrophobic behaviour, hence the drastically high oil measurements. It is notable that beyond a certain coating thickness, the surface likely transitions to a Wenzel state in places, where water and oil actually wet the rough surface rather than beading off, nullifying the benefit of the hydrophobic chemistry. These findings highlight an important principle for engineered oil-water separation materials: more coating is not always better. There exists an optimum in surface modification – here, one well-distributed nanoparticle layer – that achieves the desired low surface energy and appropriate roughness. Exceeding this optimum can create surface flaws (like cracks, clusters, or blockages) that harm performance. Practically, this means that to enhance oil rejection efficiency, one should focus on achieving a uniform nanoparticle coverage rather than simply maximizing the number of coating layers. The results also underscore the need for careful control of nanoparticle deposition techniques to avoid clustering. For instance, if multiple layers are needed for other reasons (e.g. durability), one might explore methods to sinter or remove excess particles after each layer to maintain surface uniformity. Additionally, the extreme failures at the third and fourth coating suggest that an oversaturated hydrophobic surface can even exacerbate oil pollution in water, possibly by shedding oil or losing the filtering function entirely.

Table 3. Effect of nanoparticle coating layers on quartz surface morphology and oil-water separation performance

Quartz Surface Condition	Residual Oil in Water (mg/L)	SEM-Observed Surface Features	Separation Performance
Raw (Uncoated)	1859.8	Very rough, uneven native surface; contaminants present; hydrophilic silica exposed.	Very poor: No oil repellency – high oil carryover due to lack of hydrophobicity.
Washed (Cleaned)	1583.7	Cleaner and somewhat smoother surface (impurities removed); still intrinsic quartz texture (hydrophilic).	Very poor: Slight improvement from raw (fewer fouling sites) but still ineffective without a hydrophobic coating.
1st Nanoparticle Coating	29.3	Uniform monolayer of hydrophobic NPs; minimal clustering; consistent nano-roughness (lotus-like).	Excellent: Drastic reduction in oil content. Uniform hydrophobic surface enables optimal oil rejection and water passes clean.
2nd Nanoparticle Coating	547.4	Increased NP density; beginning of small clusters; higher roughness with minor unevenness.	Good (but lower): Hydrophobicity maintained overall, but slight loss of uniformity causes some oil breakthrough (performance declines vs. 1st coat).
3rd Nanoparticle Coating	27177	Heavy NP build-up; pronounced clustering and multilayer islands; very rough and irregular.	Extremely poor: Surface oversaturated and uneven – oil-water separation largely fails as oil traverses or is released (oil in water skyrockets).
4th Nanoparticle Coating	73439.7	Oversaturated NP layer; severe clustering with some areas over-coated and others less covered; chaotic morphology.	Worst: Separation effectively collapses; surface morphology and clogging cause more oil in water than even initial state.

In summary, the progression from Figures 4 to 9 demonstrates that transforming raw quartz into an effective oil-water separator is achievable with a single-layer nanoparticle coating that renders the surface superhydrophobic and uniformly rough. Washing the quartz is an essential preparatory step, but it is the first hydrophobic nanocoating that yields the huge leap in performance (oil in water down to ~29 mg/L). Each additional coating beyond the first then compromises the surface structure and thus the separation efficiency, with the fourth coating performing worst of all. This comprehensive SEM analysis, reinforced by quantitative oil content data, provides a clear guidance: for quartz-based oil-water separation media, one good coating is optimal, and excessive layering is detrimental. These insights could help in optimizing coating processes for practical wastewater treatment applications, balancing the need for hydrophobicity, surface roughness, and material stability to achieve the best possible separation outcomes.

4. CONCLUSION

This study has successfully demonstrated the potential of hydrophobic nanoparticle coatings to significantly enhance the oil-water separation efficiency of quartz-based filtration media. The experimental findings reveal that the application of a single, uniformly distributed layer of hydrophobic nanoparticles on quartz particles dramatically improves surface wettability and oil rejection capacity. SEM analysis confirmed that this first coating achieved an optimal balance of surface roughness and nanoparticle coverage, creating a homogenous, superhydrophobic surface capable of reducing oil and grease content in the permeate to as low as 29.3 mg/L.

In contrast, subsequent coatings—ranging from the second to the fourth layer—introduced surface irregularities, nanoparticle clustering, and excessive roughness. These morphological changes disrupted the uniformity of the hydrophobic layer, thereby diminishing the quartz's separation performance. As observed through both SEM characterization and oil-and-grease analysis, excessive nanoparticle layering not only failed to enhance performance but in fact led to significant declines in efficiency, with oil content in the filtrate rising exponentially.

The mathematical models developed in this study provided a quantitative means to evaluate key performance indicators such as oil rejection efficiency, nanoparticle uniformity, and surface morphology. These models reinforced the conclusion that a single, well-applied hydrophobic coating maximizes the separation capability of the quartz material. Overall, this work presents a low-cost, scalable, and environmentally sustainable approach to oily wastewater treatment using naturally abundant quartz materials enhanced by optimized surface engineering.

Future research should focus on critical areas to further optimize the performance and scalability of nanoparticle-coated quartz materials for oil-water separation:

Optimization of Coating Parameters: Further studies are needed to determine the ideal nanoparticle size, material type, and surface chemistry that yield the highest hydrophobicity

without inducing clustering or surface saturation. Investigating alternative hydrophobic agents, such as fluorine-free or bio-based nanoparticles, could offer improved environmental compatibility.

ACKNOWLEDGMENT

This work is supported by the National Research Foundation (NRF) of South Africa (grant number NFSG240507217649), through the FirstRand Empowerment Foundation (FREF) under the Black Academics Advancement Programme (BAAP). The authors also express their sincere gratitude to the University of South Africa (UNISA) for support provided through the University Staff Doctoral Programme (USDP) grant.

REFERENCES

[1] Khalefah, A.R.M., Omran, I.I., Al-Waily, M.J.M. (2024). An investigation on the environmental impact of petroleum refinery effluent on soil pollution. International Journal of Environmental Impacts, 7(1): 41-46. https://doi.org/10.18280/ijei.070105

[2] Mehrasa, S., Hoseinzadeh, M., Mohammadpour, S., Saboor, F.H. (2024). Decontamination of oily and micro-pollutant loaded wastewater using metal organic framework. Reference Module in Materials Science and Materials Engineering.

[3] Spengler, S., Heskett, M. (2023). Impact to stream water quality from sewage exfiltration and legacy on-site disposal systems on the island of O'Ahu, Hawaii. International Journal of Environmental Impacts, 6(1): 13-23. https://doi.org/10.18280/ijei.060103

[4] Alqassab, M., Waheed, A., Baig, U., Hasan, S.W., Aljundi, I.H. (2024). Enhancing the efficiency of polymeric-inorganic composite mixed matrix membrane for oil/water separation via SiC decoration in the polyvinyl alcohol/glutaraldehyde framework. Results in Chemistry, 7: 101483. https://doi.org/10.1016/j.rechem.2024.101483

[5] Baig, U., Waheed, A. (2023). An efficient and simple strategy for fabricating a polypyrrole decorated ceramic-polymeric porous membrane for purification of a variety of oily wastewater streams. Environmental Research, 219: 114959. https://doi.org/10.1016/j.envres.2022.114959

[6] Baig, U., Usman, J., Abba, S.I., Yogarathinam, L.T., Waheed, A., Bafaqeer, A., Aljundi, I.H. (2024). Insight into soft chemometric computational learning for modelling oily-wastewater separation efficiency and permeate flux of polypyrrole-decorated ceramic-polymeric membranes. Journal of Chromatography A, 1725: 464897. https://doi.org/10.1016/j.chroma.2024.464897

[7] Hao, M., Zhang, T., Hu, X., Chen, Z., Yang, B., Wang, X., Liu, Y. (2023). Facile, green and scalable preparation of low-cost PET-PVDF felts for oil absorption and oil/water separation. Journal of Hazardous Materials, 448: 130804. https://doi.org/10.1016/j.jhazmat.2023.130804

[8] Yang, Y., Jiang, X., Goh, K.L., Wang, K. (2021). The separation of oily water using low-cost natural materials: Review and development. Chemosphere, 285: 131398. https://doi.org/10.1016/j.chemosphere.2021.131398

[9] Pan, J., Ge, Y. (2023). Low-cost and high-stability superhydrophilic/underwater superoleophobic NaA zeolite/copper mesh composite membranes for oil/water separation. Surfaces and Interfaces, 37: 102703. https://doi.org/10.1016/j.surfin.2023.102703

[10] Chen, M., Wang, Z., Weng, S., Yue, J., Wang, Z., Zhang, H., Fu, Q. (2024). Submicron-ultrathin PE/PDVB composite membrane for efficient oil/water separation. Journal of Membrane Science, 701: 122701. https://doi.org/10.1016/j.memsci.2024.122701

[11] Fan, Z., Zhou, S., Mao, H., Li, M., Xue, A., Zhao, Y., Xing, W. (2021). A novel ceramic microfiltration membrane fabricated by anthurium andraeanum-like attapulgite nanofibers for high-efficiency oil-in-water emulsions separation. Journal of Membrane Science, 630: 119291. https://doi.org/10.1016/j.memsci.2021.119291

[12] Xiang, B., Gong, J., Sun, Y., Yan, W., Jin, R., Li, J. (2024). High permeability PEG/MXene@ MOF membrane with stable interlayer spacing and efficient fouling resistance for continuous oily wastewater purification. Journal of Membrane Science, 691: 122247. https://doi.org/10.1016/j.memsci.2023.122247

[13] Bombom, M., Zaman, B.T., Bozyiğit, G.D., Şaylan, M., Bayraktar, A., Arvas, B., Bakırdere, S. (2023). T-cut slotted quartz tube-atom trap strategy for the on-line preconcentration of thallium in well water samples. Measurement, 220: 113363. https://doi.org/10.1016/j.measurement.2023.113363

[14] Wang, T., Cao, W., Wang, Y., Qu, C., Xu, Y., Li, H. (2023). Surface modification of quartz sand: A review of its progress and its effect on heavy metal adsorption. Ecotoxicology and Environmental Safety, 262: 115179. https://doi.org/10.1016/j.ecoenv.2023.115179

[15] Villalobos, L.F., Pataroque, K.E., Pan, W., Cao, T., Kaneda, M., Violet, C., Elimelech, M. (2023). Orientation matters: Measuring the correct surface of polyamide membranes with quartz crystal microbalance. Journal of Membrane Science Letters, 3(2): 100048. https://doi.org/10.1016/j.memlet.2023.100048

[16] Wang, J., Yu, Z., Xiao, X., Chen, Z., Huang, J., Liu, Y. (2023). A novel hydroxyapatite super-hydrophilic membrane for efficient separation of oil-water emulsions, desalting and removal of metal ions. Desalination, 565: 116864. https://doi.org/10.1016/j.desal.2023.116864

[17] Kallem, P., Pandey, R.P., Hegab, H.M., Gaur, R., Hasan, S.W., Banat, F. (2022). High-performance thin-film composite forward osmosis membranes with hydrophilic PDA@ TiO2 nanocomposite substrate for the treatment of oily wastewater under PRO mode. Journal of Environmental Chemical Engineering, 10(3): 107454. https://doi.org/10.1016/j.jece.2022.107454

[18] Han, L., Shen, L., Lin, H., Huang, Z., Xu, Y., Li, R., Teng, J. (2023). 3D printing titanium dioxide-acrylonitrile-butadiene-styrene (TiO2-ABS) composite membrane for efficient oil/water separation. Chemosphere, 315: 137791. https://doi.org/10.1016/j.chemosphere.2023.137791

[19] Kumari, P., Chauhan, P., Kumar, A. (2022). Superwetting materials for modification of meshes for oil/water separation. In Oil−Water Mixtures and Emulsions, Volume 2: Advanced Materials for

Separation and Treatment, pp. 1-23. https://doi.org/10.1021/bk-2022-1408.ch001
[20] Hou, K., Jin, K., Fan, Z., Du, P., Ji, Y., Wang, J., Cai, Z. (2023). Facile fabrication of fabric-based membrane for adjustable oil-in-water emulsion separation, suspension filtration and dye removal. Separation and Purification Technology, 323: 124467. https://doi.org/10.1016/j.seppur.2023.124467
[21] Zhang, X., Hu, C., Lin, J., Yin, H., Shi, J., Tang, J., Ren, K. (2022). Fabrication of recyclable, superhydrophobic-superoleophilic quartz sand by facile two-step modification for oil-water separation. Journal of Environmental Chemical Engineering, 10(1): 107019. https://doi.org/10.1016/j.jece.2021.107019
[22] Wang, Z., Cui, Z., Qi, X., Shao, Y., Zhang, J., Zhao, Y., Chen, Y. (2024). Constructing superhydrophilic/superhydrophobic Janus membrane assisted by dual-interface-confined strategy for on-demand oil-in-water and water-in-oil emulsions separation. Separation and Purification Technology, 350: 127846. https://doi.org/10.1016/j.seppur.2024.127846
[23] Feng, S., Xu, M., Leng, C., Ma, Q., Wang, L., Meng, H., Gong, X. (2024). Bio-inspired superhydrophobic fiber membrane for oil-water separation and non-destructive transport of liquids in corrosive environments. Journal of Membrane Science, 705: 122852. https://doi.org/10.1016/j.memsci.2024.122852
[24] Zhang, S., Li, Y., Yuan, Y., Jiang, L., Wu, H., Dong, Y. (2024). Biomimetic hydrophilic modification of poly (vinylidene fluoride) membrane for efficient oil-in-water emulsions separation. Separation and Purification Technology, 329: 125227. https://doi.org/10.1016/j.seppur.2023.125227
[25] Ding, J., Zhang, X., Chen, H. (2024). Fabrication and oil-water separation properties of cerium oxide coated zirconium oxide composite membranes. Colloids and Surfaces A: Physicochemical and Engineering Aspects, 683: 133069. https://doi.org/10.1016/j.colsurfa.2023.133069
[26] Xie, A., Wu, Y., Liu, Y., Xue, C., Ding, G., Cheng, G., Pan, J. (2022). Robust antifouling NH2-MIL-88B coated quartz fibrous membrane for efficient gravity-driven oil-water emulsion separation. Journal of Membrane Science, 644: 120093. https://doi.org/10.1016/j.memsci.2021.120093
[27] Liu, H., Xie, J., Zhao, J., Wang, R., Qi, Y., Lv, Z., Sun, S. (2024). Construction of gradient SA-TiO2 hydrogel coated PVDF-g-IL fibre membranes with high hydrophilicity and self-cleaning for the efficient separation of oil-water emulsion and dye wastewater. Journal of Membrane Science, 697: 122580. https://doi.org/10.1016/j.memsci.2024.122580
[28] Sob, P.B., Alugongo, A.A., Tengen, T.B. (2020). The stochastic effect of nanoparticles inter-separation distance on membrane wettability during oil/water separation. International Journal of Engineering Research and Technology, 13(5): 842-866. https://doi.org/10.37624/ijert/13.5.2020.842-866
[29] Chen, M., Heijman, S.G., Rietveld, L.C. (2024). Ceramic membrane filtration for oily wastewater treatment: Basics, membrane fouling and fouling control. Desalination, 583: 117727. https://doi.org/10.1016/j.desal.2024.117727
[30] Zhong, J., Xin, Y. (2023). Preparation, compatibility and barrier properties of attapulgite/poly (lactic acid)/thermoplastic starch composites. International Journal of Biological Macromolecules, 242: 124727. https://doi.org/10.1016/j.ijbiomac.2023.124727
[31] Zhang, T., Zhao, J., Kong, D., Zhou, J., Wang, X., Wei, B. (2024). Solvent-responsive switching wettability of superoleophobic/superhydrophilic quartz sand filter medium facilitates rapidly oil/water separation and demulsification. Colloids and Surfaces A: Physicochemical and Engineering Aspects, 697: 134418. https://doi.org/10.1016/j.colsurfa.2024.134418
[32] Zhao, Z., Dong, J., Dong, W., Wang, L., Wang, P., Zhou, Y., Li, D. (2023). PI nanofiber membranes with pH-responsive wettability fabricated through solution blow spinning for efficient on-demand oil-water separation. Journal of Environmental Chemical Engineering, 11(6): 111565. https://doi.org/10.1016/j.jece.2023.111565
[33] Yan, D., Zhao, Y., Zhang, S., Wang, X., Ning, X. (2024). Robustly wettability-switchable polylactic acid nanofibrous membranes bearing CO2-responsive trigger and emulsion breaker for versatile oil–water separation. Chemical Engineering Journal, 493: 152679. https://doi.org/10.1016/j.cej.2024.152679
[34] Liang, Y., Yang, E., Kim, M., Kim, S., Kim, H., Byun, J., Choi, H. (2023). Lotus leaf-like SiO2 nanofiber coating on polyvinylidene fluoride nanofiber membrane for water-in-oil emulsion separation and antifouling enhancement. Chemical Engineering Journal, 452: 139710. https://doi.org/10.1016/j.cej.2022.139710
[35] Li, Y., Fan, T., Cui, W., Wang, X., Ramakrishna, S., Long, Y. (2023). Harsh environment-tolerant and robust PTFE@ ZIF-8 fibrous membrane for efficient photocatalytic organic pollutants degradation and oil/water separation. Separation and Purification Technology, 306: 122586. https://doi.org/10.1016/j.seppur.2022.122586
[36] Chai, J., Wang, G., Zhang, A., Zhao, G., Park, C.B. (2024). Superhydrophobic nanofibrous polytetrafluoroethylene and composite membranes with tunable adhesion for micro-droplet manipulation, self-cleaning and oil/water separation. Journal of Environmental Chemical Engineering, 12(2): 112355. https://doi.org/10.1016/j.jece.2024.112355
[37] Bonyadi, E., Ashtiani, F.Z., Ghorabi, S., Niknejad, A.S. (2022). Bio-inspired hybrid coating of microporous polyethersulfone membranes by one-step deposition of polydopamine embedded with amino-functionalized SiO2 for high-efficiency oily wastewater treatment. Journal of Environmental Chemical Engineering, 10(1): 107121. https://doi.org/https://doi.org/10.1016/j.jece.2021.107121
[38] Ahmed, F.U., Purkayastha, D.D. (2022). PVDF@ ZnO membrane for its potential application in oil/water separation. Materials Today: Proceedings, 68: 177-180. https://doi.org/10.1016/j.matpr.2022.07.236
[39] Aghaei, A., Suresh, K., Firouzjaei, M.D., Elliott, M., Rahimpour, A., Sadrzadeh, M. (2023). Hybrid/integrated treatment technologies for oily wastewater treatment. In Advanced Technologies in Wastewater Treatment, pp. 377-419. https://doi.org/10.1016/B978-0-323-99916-8.00002-X

[40] Omar, N.M.A., Othman, M.H.D., Tai, Z.S., Jaafar, J., Rahman, M.A., Puteh, M.H., Li, T. (2024). Fabrication and characterization of a novel mullite-stainless steel composed hollow fibre membrane for oil/water separation. Ain Shams Engineering Journal, 15(1): 102260. https://doi.org/10.1016/j.asej.2023.102260

[41] Yahaya, N.Z.S., Azmi, N.F.A.N., Rahman, M.A., Abas, K.H., Othman, M.H.D., Jaafar, J. (2024). Antifouling and self-cleaning photocatalytic membranes in oily wastewater treatment. In Advanced Ceramics for Photocatalytic Membranes, pp. 481-497. https://doi.org/10.1016/B978-0-323-95418-1.00018-5

[42] Wang, X., Sun, K., Zhang, G., Yang, F., Lin, S., Dong, Y. (2022). Robust zirconia ceramic membrane with exceptional performance for purifying nano-emulsion oily wastewater. Water Research, 208: 117859. https://doi.org/10.1016/j.watres.2021.117859

[43] Cai, J., Liu, S., Gao, C., Ji, S., Xing, Y. (2023). A high-toughness anti-pollution polyethersulfone membrane for efficient separation of oil-in-water emulsions. Journal of Environmental Chemical Engineering, 11(1): 108980. https://doi.org/10.1016/j.jece.2022.108980

[44] Hudaib, B., Al-Qodah, Z., Abu-Zurayk, R., Waleed, H., Omar, W. (2024). Fabrication of blended cellulose acetate/poly-pyrrole ultrafiltration membranes for crude oil wastewater separation. Case Studies in Chemical and Environmental Engineering, 9: 100692. https://doi.org/10.1016/j.cscee.2024.100692

[45] Wu, L., Gao, Y., Xu, X., Deng, J., Liu, H. (2024). Excellent coagulation performance of polysilicate aluminum ferric for treating oily wastewater from Daqing gasfield: Responses to polymer properties and coagulation mechanism. Journal of Environmental Management, 356: 120642. https://doi.org/https://doi.org/10.1016/j.jenvman.2024.120642

[46] Ning, D., Lu, Z., Tian, C., Yan, N., Xie, F., Li, N., Hua, L. (2023). Superwettable cellulose acetate-based nanofiber membrane with spider-web structure for highly efficient oily water purification. International Journal of Biological Macromolecules, 253: 126865. https://doi.org/10.1016/j.ijbiomac.2023.126865

[47] Mao, H., Fan, W., Cao, H., Chen, X., Qiu, M., Verweij, H., Fan, Y. (2022). Self-cleaning performance of in-situ ultrasound generated by quartz-based piezoelectric membrane. Separation and Purification Technology, 282: 120031. https://doi.org/10.1016/j.seppur.2021.120031

[48] Manouchehri, M. (2024). A comprehensive review on state-of-the-art antifouling super (wetting and anti-wetting) membranes for oily wastewater treatment. Advances in Colloid and Interface Science, 323: 103073. https://doi.org/10.1016/j.cis.2023.103073

[49] Alhammad, F., Ali, M., Yekeen, N.P., Ali, M., Hoteit, H., Iglauer, S., Keshavarz, A. (2023). Effect of methylene blue on wetting characteristics of quartz/H2/brine systems: Implication for hydrogen geological storage. Journal of Energy Storage, 72: 108340. https://doi.org/10.1016/j.est.2023.108340

[50] Li, K., Feng, G., Li, G., Zhang, Z., Xiang, J., Jiao, F., Zhao, H. (2024). Structurally integrated janus polylactic acid fibrous membranes for oil-water separation. Journal of Water Process Engineering, 68: 106525. https://doi.org/10.1016/j.jwpe.2024.106525